Development of a rabbit model of Adenosine triphosphate-induced monocular retinal degeneration for optimization of retinal prostheses*

Hallur Reynisson, Lisa Nivison-Smith, Nigel H Lovell, *Fellow, IEEE*, Michael Kalloniatis, and Mohit N Shivdasani, *Senior Member, IEEE*

***Abstract*— Optimization of retinal prostheses requires preclinical animal models that mimic features of human retinal disease, have appropriate eye sizes to accommodate implantable arrays, and provide options for unilateral degeneration so as to enable a contralateral, within-animal control eye. In absence of a suitable non-human primate model and shortcomings of our previous feline model generated through intravitreal injections of Adenosine Triphosphate (ATP), we aimed in the present study to develop an ATP induced degeneration model in the rabbit. Six normally sighted Dutch rabbits were monocularly blinded with this technique. Subsequent retinal degeneration was assessed with optical coherence tomography, electroretinography, and histological assays. Overall, there was a 42% and 26% reduction in a-wave and oscillatory potential amplitudes in the electroretinograms respectively, along with a global decrease in retinal thickness, with increased variability. Qualitative inspection also revealed that there were variable levels of retinal degeneration and remodeling both within and between treated eyes, mimicking the disease heterogeneity observed in retinitis pigmentosa. These findings confirm that ATP can be utilized to unilaterally induce blinding in rabbits and, potentially present an ideal model for future cortical recording experiments aimed at optimizing vision restoration strategies.**

***Clinical Relevance*— A rapid, unilaterally induced model of retinal degeneration in an animal with low binocular overlap and large eyes will allow for clinically valid recordings of downstream cortical activity following retinal stimulation. Such a model would be highly beneficial for the optimization of clinically appropriate vision restoration approaches.**

I. Introduction

The development and optimization of retinal prostheses that use electrical stimulation to activate surviving retinal neurons via implanted electrodes, requires an animal model that (1) closely mimics retinal features seen in human retinitis pigmentosa (i.e. widespread photoreceptor degeneration and remodeling), and (2) has eye dimensions that allow for the implantation of clinically relevant electrode sizes and electrode array positioning [1]. Ideally, such a model should also be unilaterally blind in order to maintain a healthy control eye within the same animal, so that neural responses, particularly those evoked in the visual cortex, from healthy and degenerate retinal stimulation can be directly compared and various stimulation strategies optimized before proceeding to human trials.

Few models currently fit the above requirements. Genetic models in many species including rodents, rabbits, cats and dogs mimic human disease well by design, but are typically bilateral and slow progressing making them uneconomical, as achieving sufficient retinal degeneration for implantation takes long time periods [2]. Chemically-induced models of retinal degeneration offer a more rapid model but have been associated with adverse systemic affects [3] and increased cancer risk through DNA interactions [4].

In an attempt to address the above criteria, we previously generated a large animal model of induced retinal degeneration through intravitreal injections of adenosine triphosphate (ATP) in felines [1]. This model demonstrated heterogeneous retinal degeneration reminiscent of human disease with tunable degeneration based on ATP concentration and no systemic effects [5]. The feline model eye size also allowed for successful implantation of multi-electrode arrays and cortical recording [6].

However, the binocularity of the feline visual system means that cortical areas of the ATP-induced feline model potentially remain unaltered following monocular retinal degeneration through compensation by the contralateral healthy control eye [7-8]. Thus, neural responses gathered from cortical areas of the feline model might not be representative of humans who are bilaterally blind, regardless of the high symmetry at the level of the retina.

The rabbit visual system demonstrates minimal binocular overlap and therefore may be a more suitable large eye model to study evoked cortical responses to electrical stimulation from a unilaterally degenerated retina. Previous studies have developed rabbit models through chemically induced retinal degeneration [9-10]. These models however pose several challenges including the need for vitrectomies, increased risks of the animals developing cancers [11], and major alterations in ocular circulation following treatment [9]. Thus, a safe and validated rabbit model of unilateral retinal degeneration is still lacking. The aim of this study was therefore to develop a

*Research supported by UNSW Scientia PhD scholarship (H. Reynisson), UNSW infrastructure funding (M.N. Shivdasani), and UNSW Scientia program (L. Nivison-Smith).

H. Reynisson is UNSW Sydney, Kensington, NSW, 2052, AUS (phone: 0427-102-480; e-mail: h.reynisson@unsw.edu.au).

M. N. Shivdasani is with UNSW Sydney, Kensington, NSW, 2052, AUS (e-mail: m.shivdasani@unsw.edu.au).

M. Kalloniatis is with Deakin University, Burwood, VIC, 3125, AUS (e-mail: michael.kalloniatis@deakin.edu.au).

L. Nivison-Smith is with UNSW Sydney, Kensington, NSW, 2052, AUS (e-mail: l.nivison-smith@unsw.edu.au).

N. H. Lovell is with UNSW Sydney, Kensington, NSW, 2052, AUS (e-mail: n.lovell@unsw.edu.au).

Correspondence to: m.shivdasani@unsw.edu.au

protocol to generate a rabbit model of ATP-induced retinal degeneration. This model could then be used in future cortical recording experiments aimed at optimizing vision restoration strategies.

II. Methods

A. Ethics Statement

All procedures were conducted in accordance with the ARVO statement for the Use of Animals in Ophthalmic and Vision Research and approved by the Animal Ethics Committee of UNSW Sydney (ACEC #20-61A).

B. Animals

Normal sighted Dutch rabbits (n=6) were housed in pens of minimal size 2.25 m^2. Rabbits were provided with food and water *ad libitum*, as well as enrichment. Pens were kept at an artificial light schedule of 12 hours of light on followed by 12 hours of lights off.

C. Anesthesia

Anesthesia pre-medication was provided by a combined intramuscular injection of Ketamine (15 mg/kg), Medetomidine (0.04 mg/kg), and Midazolam (0.2 mg/kg). Further induction was provided after catheterization through an intravenous bolus of Propofol (3-10 mg/kg), then maintained through continuous rate infusion delivery (3-60 mg/kg/hr) using a syringe pump. The animal was given 100% oxygen and monitored for oxygen levels, heart- and respiratory rate (Anitek C50-V vet monitor), and temperature through a rectal thermometer.

D. ATP induced degeneration

A 0.33 M solution of ATP was administered as a single intravitreal injection (50 µL) to achieve a final vitreal concentration of 11 mM. Injections were given whilst the animal was under a surgical plane of anesthesia. Contralateral control eyes were injected with equivolumes of saline (0.9% w/v NaCl). Eyes were injected, approximately 5 mm posterior to the limbus at a 45-degree angle in order to avoid the lens, using a 30G needle attached to a Hamilton syringe (Hamilton Company, Reno, NV). Test eyes were selected at random. All intravitreal injections included 0.05 mL of Dexamethasone to reduce the inflammatory response due to ATP.

Following the procedure, topical Chloramphenicol (0.5%) and Prednisolone Forte (0.5%) was applied to the eyes every 15 mins until the animal recovered from anesthesia to minimize infection and inflammation respectively.

E. In vivo assessments

In vivo assessments were conducted at baseline (pre-injection) and experimental endpoint (2 weeks post-injection). Retinal structure was examined by optical coherence tomography (OCT), with a scan depth of 2-2.5 mm and a 5 µm axial resolution. Standard color fundus imaging was performed along with imaging using an infrared laser scanning ophthalmoscope (Roland Consult Imaging and Electrophysiology System, Germany).

Retinal function was assessed using The International Society for Clinical Electrophysiology of Vision (ISCEV: www.iscev.org) standard full-field electroretinogram (ERG) using a RETI-map animal system (Roland Consult Imaging and Electrophysiology System, Germany). Briefly, animals were dark-adapted for 1 hour under general anesthesia. Eyes were then locally anaesthetized with Proxymetacaine (0.5%), dilated with Tropicamide (1%) and gold ring electrodes placed on the corneas. Full-field flashes were presented following the ISCEV standard following 15 minutes exposure to light within the Ganzfeld.

F. Tissue collection and histology

Following *in vivo* assessments at the experimental end-point, animals were euthanized with an overdose of sodium pentobarbital (120 mg/kg, i.v.) whilst under anesthesia. Eyes were then enucleated and the retina isolated and fixed in either 4% paraformaldehyde for 30 minutes or Davidson's fixative for 24 hours [12]. Retinae were then washed in 0.1 M phosphate buffer, equilibrated in graded sucrose (10% - 30% w/v), frozen embedded in optimal cutting temperature compound (Tissue-Tek; Torrance, CA, USA) and cryo-sectioned into sections of 12 µm thickness.

H&E staining was performed as described in [13]. Immunostaining was performed as described in [14]. Briefly, retinal sections were blocked for 60 minutes with 6% (v/v) goat serum, 1% (w/v) bovine serum albumin, 0.1% (v/v) Triton-X then incubated overnight at 4˚C with Anti-Rhodopsin antibody (dilution 1:1000, ab98887; Abcam; Cambridge, United Kingdom). Primary antibody was detected with anti-mouse AlexaFluor 488 (Thermo Fisher Scientific, Oregon, USA) at a 1:500 dilution for 2 h at room temperature. All antibody dilutions were made in 3% (v/v) goat serum, 1% (w/v) bovine serum albumin, 0.1% (v/v) Triton-X. Counterstaining was performed with 2-(4-amidinophenyl)-1H -indole-6-carboxamidine (DAPI) diluted 1:1000 in MilliQ water. All samples were mounted in Citifluor mounting media (ProSciTech, QLD, Australia). Sections were imaged using a Vectra Polaris Slide Scanner (PerkinElmer, Waltham, MA, United States).

G. Data analysis

OCT images were analyzed qualitatively. Retinal thickness from histology sections were measured using Phenochart (Phenochart Whole Slide Viewer, v1.1; Akoya Biosciences, Marlborough, MA, United States). Retinal thickness variability was measured as the normalized variability across ten evenly spaced cross sections within a 1 mm window for the entire length of each retinal section.

ERG recordings were assessed for maximum a-wave, b-wave, and oscillatory potentials amplitudes using custom MATLAB® (R2020b, v9.9.0, Mathworks, Natrick, MA, USA) scripts. Data was analyzed using the two-sample t-test. Statistical analyses were performed using MATLAB® and the Statistics and Machine Learning Toolbox v12.0.

III. Results

A. Structural evidence of retinal degeneration

ATP induced variable levels of retinal thinning both within treated eyes (Figure 1B, E, boxed areas) and between treated eyes of different animals (Figure 1C vs 1F) at two weeks post-injection. *En face* and OCT images both showed no evidence of retinal detachment post-injection. OCT images of all control

eyes showed uniform thickness, with thickness as a function of eccentricity (*data not shown)*.

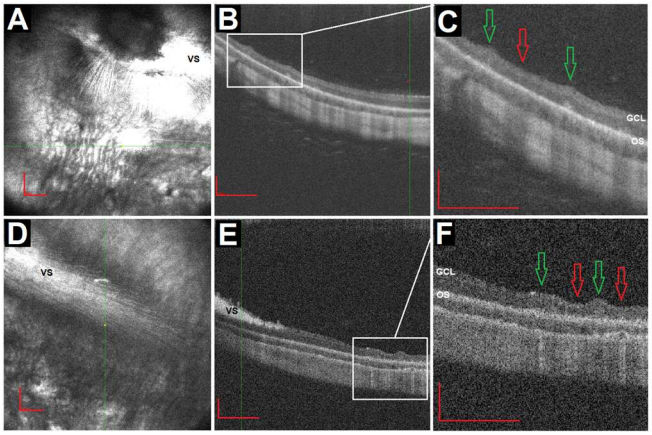

Figure 1. In vivo images of ATP-treated retinae of two separate rabbits two weeks post injection. (A) Fundus, (B) OCT scan and (C) magnified OCT scan of retina of rabbit 1 taken temporal to the optic disc in the frontal plane. (D) Fundus, (E) OCT scan and (F) magnified OCT scan of retina of rabbit 2 taken inferior to the optic disc in the vertical plane. Green and red arrows indicate normal and degenerated photoreceptor regions respectively based on Ahn et al., 2019 [15], which showed the retina "sinks" where photoreceptors have degenerated (red arrows) along with a complete change of ERG signal. Abbreviations: GCL, Ganglion Cell Layer; OS, Outer Segments; VS, Visual Streak. Scale bar is 200µm.

B. Functional evidence of retinal degeneration

ATP treated eyes showed a significant average reduction of 42±16% in a-wave amplitude compared to contralateral control eyes across all light levels (Figure 2A-B, E; $p < 0.01$), and a significant 26.2±9.7% reduction in oscillatory potential (OP) amplitude versus control (Figure 2C-E; $p < 0.05$). B-wave amplitudes were also reduced by 13±14%, but this reduction was not significant (Figure 2E; $p = 0.4582$).

C. Histological evidence of retinal degeneration

H&E staining confirmed variable levels of retinal degeneration within and between ATP treated eyes as seen on OCT. This included areas of mild retinal degeneration with no alteration in lamination nor thickness (Figure 3B) similar to control (Figure 3A) to areas of severe retinal degeneration with poor lamination of nuclear and synaptic layers (Figure 3C). Interestingly, within mild retinal degeneration, rhodopsin redistribution into the nuclear layer and spherules was evident (Figure 3B), along with photoreceptor outer segment disruptions, and nuclei reduction in the outer nuclear layer. In severe degeneration there was absence of photoreceptor outer and inner segments, nuclear migration, and great redistribution of rhodopsin (Figure 3C).

Global quantification indicated a significant loss in total retinal thickness of 28.7% in ATP treated eyes compared to untreated eyes (Figure 3D, Control = 151.7±3.3 µm, ATP = 108.1±2.7 µm; $p < 0.01$). The variability in retinal thickness measurements was also significantly increased in ATP vs control eyes (Figure 3E, Control = 18.6±1.4%, ATP = 27.7±2.5%; $p < 0.001$).

IV. Discussion

This study successfully developed a unilateral model of retinal degeneration in the rabbit using a single intravitreal injection of ATP without systemic adverse effects.

All forms of imaging showed no evidence of retinal detachment for all eyes.

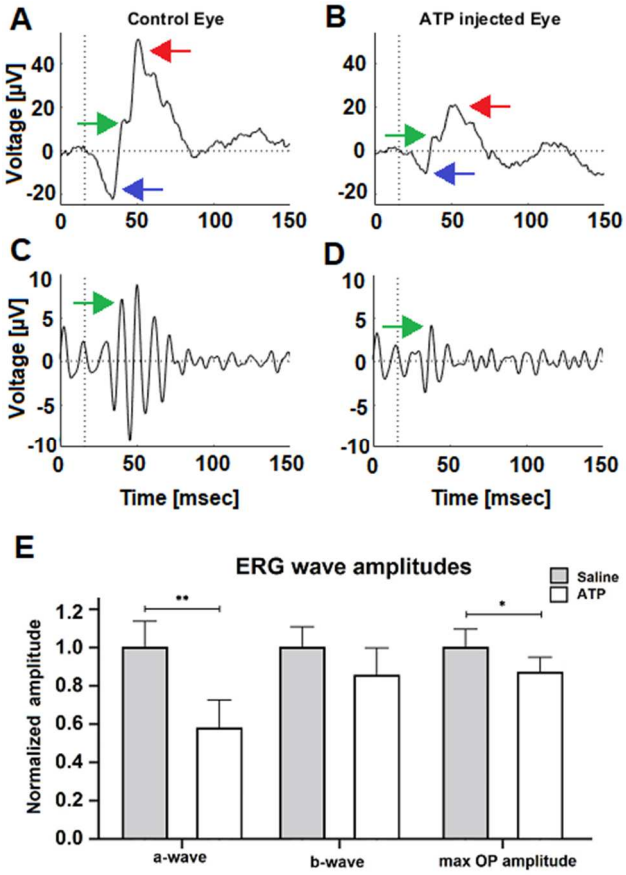

Figure 2. Representative ERG responses showing the averaged response from a dark-adapted trial (3.0 cd/m^2) for one animal two weeks post injection. (A & C) control eye. (B & D) ATP injected eye. (A-B) Unfiltered average responses. (C-D) Filtered oscillatory potentials. (E) Normalized amplitudes of the a-wave, b-wave, and maximum oscillatory potential. Control eye in grey, ATP eye in white. Blue arrows point to the a-wave, red arrows point to the b-wave, and green arrows show OPs in the unfiltered (A-B) and filtered (C-D) plots. Statistical comparisons were performed via t-test; $p \leq 0.05$, *; $p \leq 0.01$, **. Error bars represent the standard error of the mean.

Our model showed evidence of photoreceptor degeneration (based on a-wave loss) [16], and inner retinal function loss (based on oscillatory potential loss). The latter is also supported by a consistent but non-significant reduction in the b-wave amplitude, which reflects bipolar cells and Müller glia function [17]. These functional losses reflect those of human disease, particularly with degeneration beyond photoreceptors and into inner retinal layers [18] .

OCT imaging revealed regions of variable levels of degeneration. This also mimics human disease with reports of regions of healthy retina co-existing against areas of varying degrees of retinal degeneration and remodeling within the same eye [19]. Our histological results also revealed the same variability but further revealed loss of retinal lamination within the degenerate regions interspersed among stretches of seemingly healthy retina, though some sections of seemingly healthy retina had undergone early stages of degeneration as seen in the Q64ter rhodopsin mutation causing retinitis pigmentosa [20]. All of these findings are consistent with evidence in human retinitis pigmentosa.

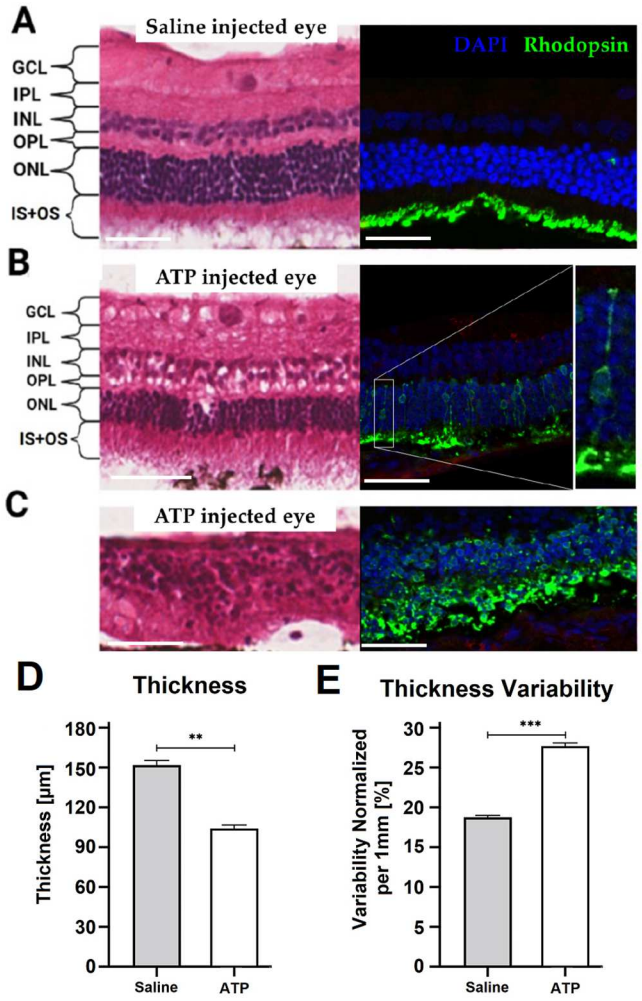

Figure 3. H&E staining (left) and Rhodopsin (green) and DAPI (blue) immunolabelling (right) images of a (A) control and (B-C) ATP injected eye of a single rabbit. From all rabbits, quantification was determined for (D) global retinal thickness and (E) normalized variability in thickness across ten evenly spaced cross sections within a 1 mm window for the entire length of each retinal section. Abbreviations: Inner and Outer Segments, IS+OS; Outer Nuclear Layer, ONL; Outer Plexiform Layer, OPL; Inner Nuclear Layer, INL; Inner Plexiform Layer, IPL; Ganglion Cell Layer, GCL. Scale bar is 50µm. Error bars represent the standard error of the mean.

V. Conclusion

This study showed that ATP delivered by a single intravitreal injection induces unilateral photoreceptor degeneration and subsequent retinal remodeling in a rabbit after two weeks. Future work with this animal model will be the study of evoked cortical responses secondary to retinal degeneration and in vision restoration intervention experiments.

Acknowledgment

The authors wish to thank Naomi Craig and Mathumathi Manoharan for technical assistance and Candice Forster for veterinary assistance.

References

[1] Aplin FP, Vessey KA, Luu CD, Guymer RH, Shepherd RK, Fletcher EL. Retinal changes in an ATP-induced model of retinal degeneration. Front Neuroanat. 2016; 10: 46.

[2] Kalloniatis, M., Nivison-Smith, L., Chua, J., Acosta, M. L., & Fletcher, E. L. (2016). Using the rd1 mouse to understand functional and anatomical retinal remodelling and treatment implications in retinitis pigmentosa: A review. Experimental eye research, 150, 106–121

[3] Siu, T., & Morley, J. (2008). Implantation of episcleral electrodes via anterior orbitotomy for stimulation of the retina with induced photoreceptor degeneration. Acta neurochirurgica, 150(5), 477–485.

[4] Maurer, E., Tschopp, M., Tappeiner, C., Sallin, P., Jazwinska, A., & Enzmann, V. (2014). Methylnitrosourea (MNU)-induced retinal degeneration and regeneration in the zebrafish: histological and functional characteristics. Journal of visualized experiments: JoVE, (92), e51909.

[5] Aplin, F. P., Luu, C. D., Vessey, K. A., Guymer, R. H., Shepherd, R. K., & Fletcher, E. L. (2014). ATP-induced photoreceptor death in a feline model of retinal degeneration. Investigative ophthalmology & visual science, 55(12), 8319–8329.

[6] Spencer, T. C., Fallon, J. B., Abbott, C. J., Allen, P. J., Brandli, A., Luu, C. D., Epp, S. B., & Shivdasani, M. N. (2018). Electrical Field Shaping Techniques in a Feline Model of Retinal Degeneration. Annual International Conference of the IEEE Engineering in Medicine and Biology Society. Annual International Conference, 2018, 1222–1225.

[7] Kaas JH, Krubitzer LA, Chino YM, Langston AL, Polley EH, Blair N,. Reorganization of retinotopic cortical maps in adult mammals after lesions of the retina. Science. 1990; 248: 229.

[8] Spear PD, Langsetmo A, Smith DC,. Age-related changes in effects of monocular deprivation on cat striate cortex neurons. J Neurophyiol. 1980: 559–580.

[9] Cho, B. J., Seo, J. M., Yu, H. G., & Chung, H. (2016). Monocular retinal degeneration induced by intravitreal injection of sodium iodate in rabbit eyes. Japanese journal of ophthalmology, 60(3), 226–237.

[10] Rösch, S., Werner, C., Müller, F., & Walter, P. (2017). Photoreceptor degeneration by intravitreal injection of N-methyl-N-nitrosourea (MNU) in rabbits: a pilot study. Graefe's archive for clinical and experimental ophthalmology = Albrecht von Graefes Archiv fur klinische und experimentelle Ophthalmologie, 255(2), 317–331.

[11] Tsubura, A., Lai, Y. C., Miki, H., Sasaki, T., Uehara, N., Yuri, T., & Yoshizawa, K. (2011). Review: Animal models of N-Methyl-N-nitrosourea-induced mammary cancer and retinal degeneration with special emphasis on therapeutic trials.

[12] Tokuda, K., Baron, B., Kuramitsu, Y., Kitagawa, T., Tokuda, N., Morishige, N., Kobayashi, M., Kimura, K., Nakamura, K., & Sonoda, K. H. (2018). Optimization of fixative solution for retinal morphology. Japanese journal of ophthalmology, 62(4), 481–490.

[13] Fischer, A. H., Jacobson, K. A., Rose, J., & Zeller, R. (2008). Hematoxylin and eosin staining of tissue and cell sections. CSH protocols, 2008, pdb.prot4986.

[14] Nivison-Smith, L., Acosta, M. L., Misra, S., O'Brien, B. J., & Kalloniatis, M. (2014). Vinpocetine regulates cation channel permeability of inner retinal neurons in the ischaemic retina. Neurochemistry international, 66, 1–14.

[15] Ahn, S. M., Ahn, J., Cha, S., Yun, C., Park, T. K., Kim, Y. J., Goo, Y. S., & Kim, S. W. (2019). The effects of intravitreal sodium iodate injection on retinal degeneration following vitrectomy in rabbits. Scientific reports, 9(1), 15696.

[16] Penn, R. D., & Hagins, W. A. (1969). Signal transmission along retinal rods and the origin of the electroretinographic a-wave. Nature, 223(5202), 201–204.

[17] Miller, R. F., & Dowling, J. E. (1970). Intracellular responses of the Müller (glial) cells of mudpuppy retina: their relation to b-wave of the electroretinogram. Journal of neurophysiology, 33(3), 323–341.

[18] Hamel C. (2006). Retinitis pigmentosa. Orphanet journal of rare diseases, 1, 40.

[19] Jones, B. W., Kondo, M., Terasaki, H., Lin, Y., McCall, M., & Marc, R. E. (2012). Retinal remodeling. Japanese journal of ophthalmology, 56(4), 289–306.

[20] Milam, A. H., Li, Z. Y., Cideciyan, A. V., & Jacobson, S. G. (1996). Clinicopathologic effects of the Q64ter rhodopsin mutation in retinitis pigmentosa. Investigative ophthalmology & visual science, 37(5), 753–765.